

THE EFFECT OF GNP ASPECT RATIO AND GNP HEAT TREATMENT ON THE PROPERTIES OF NYLON 6/GNP NANOCOMPOSITES

M. K. M. Halit¹, A. Wilkinson¹

¹School of Materials, Faculty of Engineering and Physical Sciences, The University of Manchester, Manchester, M13 9PL, UK

Email: muhammad.halit@manchester.ac.uk

¹School of Materials, Faculty of Engineering and Physical Sciences, The University of Manchester, Manchester, M13 9PL, UK

Email: arthur.wilkinson@manchester.ac.uk

Keywords: nanocomposites, graphite nanoplatelets, aspect ratio, heat treatment

Abstract

Nylon 6/ graphite nanoplatelets (PA6/GNP) nanocomposites were prepared using melt compounding using a twin screw extruder. GNP with average surface diameter of 5 μ m and 25 μ m were used in order to investigate the effect of particle aspect ratio on composite properties. It was found that at 5wt. % of GNP, there was an 8% increase of tensile modulus of composite with 25 μ m GNP compared to composite with 5 μ m GNP. However, no significant differences were observed at higher weight fractions of GNP (7 and 14 wt. %) between composites with 5 μ m GNP and 25 μ m GNP. A small increase in crystallinity and glass transition temperature were obtained with higher GNP aspect ratio at low GNP weight percentage which is in agreement with tensile modulus results. An attempt to increase the exfoliation of GNP was made through heat treatment of the as-received GNP at 160°C for 48 hours and it was found that the tensile modulus of the composites increased up to 18.5% with these heat treated GNP compared to as-received GNP. In addition, the increment in glass transition temperature also was observed with heat treated GNP. However, there were no significant changes of crystallinity between the as-received GNP and heat treated GNP.

1. Introduction

Graphene which was first isolated in 2004 has gained tremendous interest in the past decades due to its extraordinary properties [1-2]. These unique properties of graphene makes it suitable for many applications. The use of graphene as a reinforcement filler in polymer matrix has attracted considerable interest due to its mechanical, thermal and electrical properties [3]. However, the primary challenge to achieve good reinforcement is the dispersion of graphene within the polymer matrix. Graphene has the tendency to form agglomerates causing defect which led to premature failures. In order for the polymer matrix to benefit from the graphene properties, it is crucial for the graphene to be properly dispersed and distributed within the polymer matrix. The dispersion of graphene can be improved through chemical functionalisation of the graphene surface to minimize agglomeration and enhanced the graphene/polymer bond at the interface leading to effective stress transfer [4].

In addition, the cost to produce graphene is very expensive which is another challenge of using graphene. The alternative is to use a cheaper version of graphene called graphite nanoplatelets (GNP) which consist of several layers of graphene sheet is more affordable and can be mass produced [5-6]. Apart from the dispersion of graphene, the structure of graphene also plays an important role in the reinforcement of polymer nanocomposites. The effect of graphene size/aspect ratio on the physical

properties and reinforcement of polymers has recently been studied using graphite nanoplatelets and few-layer graphene [7-9].

In this study, we used two GNP with average flake diameters of 5 μm and 25 μm (denoted as AR-GNP-M5 and AR-GNP-M25) to investigate the effect of GNP aspect ratio on the thermal and mechanical properties of PA6/GNP nanocomposites. Melt compounding method was chosen to disperse the GNP into the PA6 matrix. Simple modification of GNP through heat treatment was applied to investigate the effect of heat treated GNP (HT-GNP-M25) on the nanocomposites properties compared to as received GNP (AR-GNP-M25).

2. Experimental

2.1. Materials

The matrix polymer was polyamide 6 (PA6) product name; Akulon® F136-E1 in pellet form by DSM Engineering. The nanofillers used were xGnP® graphene nanoplatelets from XG Sciences with average lateral flake diameter of 5 μm and 25 μm . Both of the nanofillers have an average thickness between 6 nm - 8 nm and were used as received for the effect of aspect ratio studies. As for GNP heat treatment, GNP M-25 was heat treated in a vacuum oven at 160°C for 48hours.

2.2 Composite preparation

The nanocomposites were prepared by melt compounding using a twin screw extruder with loadings from 3 to 14 wt.%. Prior to compounding, materials were dried for 12 hours at 80°C in a vacuum oven. Mixture of the GNP and PA6 pellets were fed into the extruder (Thermo Scientific HAAKE Minilab II micro compounder) and were cycled for 10 minutes at 260°C at a screw speed of 130 rpm before being extruded. Bone-shaped test specimens were processed by injection moulding technique using Thermo Scientific HAAKE Minijet at 280°C barrel temperature, 100°C mould temperature and 1150 bar pressure kept for 10 seconds.

2.2. Characterisation

TA Instrument DSC Q300 was used to study the melting and crystallisation behaviour of unfilled PA6 and PA6/GNP nanocomposites in nitrogen atmosphere using a heating and cooling rate of 10°C per minute between 30°C and 250°C. Samples were heated and held at 250°C for 5 minutes before cooled down to 30°C and reheated again to 250°C. The apparent crystalline content of the nanocomposites was determined using a value of 190 J/g for the heat fusion of 100% crystalline PA6.

Dynamic mechanical thermal analysis (DMTA) was performed using TA Instruments DMA Q800 in single cantilever mode at frequency of 1 Hz amplitude. Samples were dried at 80°C for 12 hours prior to test and data was obtained between -50°C and 240°C at a heating rate of 3°C per min under nitrogen flow. The glass transition temperature, T_g , was determined from the position of the $\tan \delta$ peak curve.

Tensile test were carried out at a room temperature using an Instron 4301 Universal Tester with 5 kN load cell, crosshead speed of 1 mm/min and a gauge length of 25 mm. Elastic modulus was determined from the slope of regression of the stress-strain curves between 0.05 – 0.25% strain.

3. Results and discussion

3.1 Melting and crystallisation behaviour

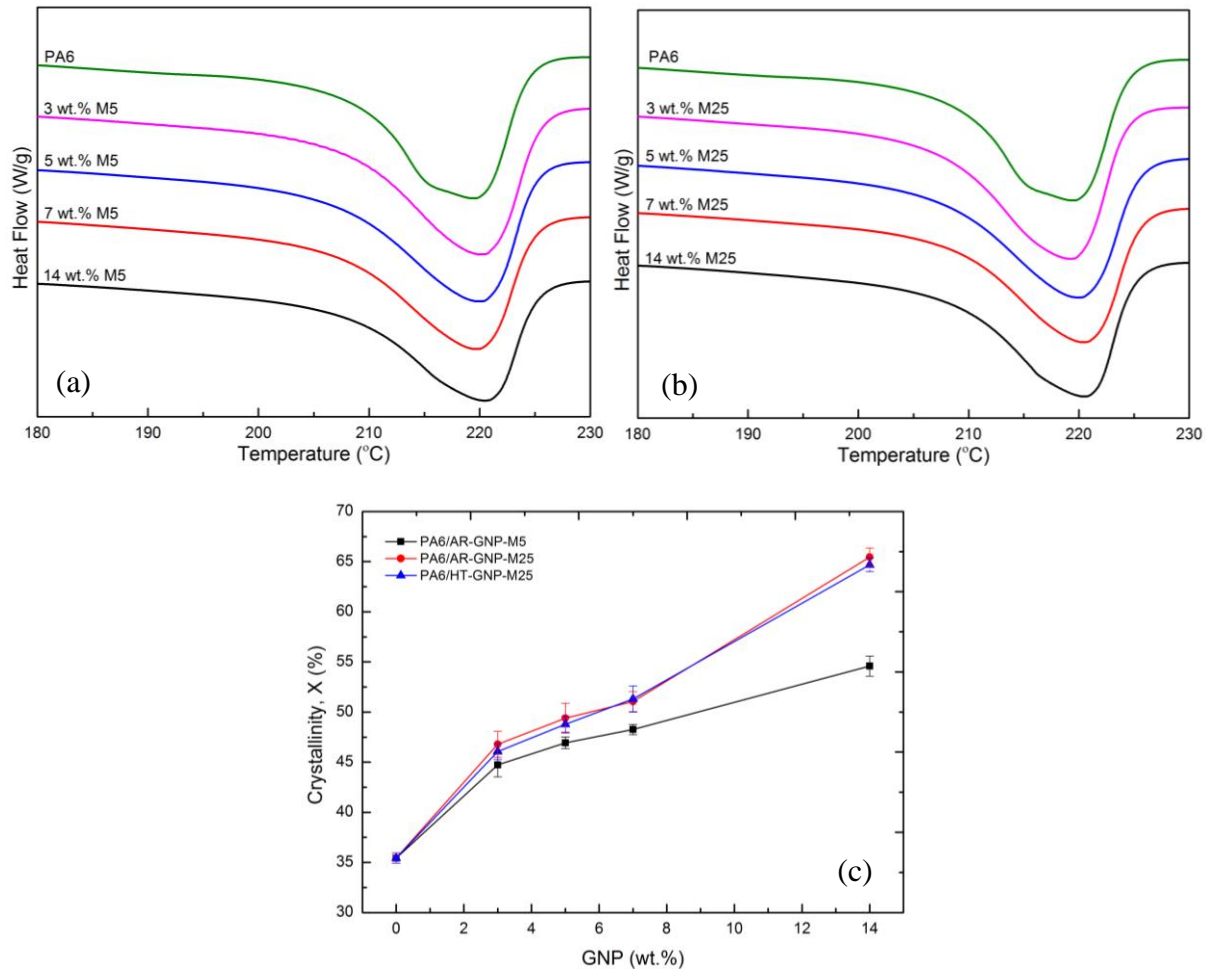


Figure 1. DSC traces for unfilled PA6 and (a) PA6/AR-GNP-M5 (b) PA6/AR-GNP-M25 and (c) crystallinity plot for PA6/GNP nanocomposites versus GNP wt.%

Thermal analysis using DSC was performed to study the effect of GNP addition on the melting and crystallisation behaviour of PA6. Figure 1 shows the DSC traces for the cooling cycle and the second heating cycle for neat PA6 and the PA6/GNP nanocomposites with AR-GNP-M5 and AR-GNP-M25. DSC traces for PA6/HT-GNP-M25 is not shown since there were no significant changes compared to PA6/AR-GNP-M25. The crystallisation temperature (T_c), melting temperature (T_m), and crystalline content (X) have been determined and listed in Table 1.

The addition of GNP significantly increased the T_c and crystallinity of PA6. The improvement in crystallinity are more apparent as the GNP addition level increases. This is indicative of strong nucleating effects by the GNP. It also clear from the melting traces in Figure 1 that there are two melting peaks in the unfilled PA6 and only one in the specimens with GNP. This second peak could be due to the melting point of some γ -form crystallites which is approximately 10°C below the the main melting peak of α -form crystals. From the WAXD results (not shown) there is a peak at $2\theta = 21.4^\circ$ observed for unfilled PA6 which represent the γ -form crystals. Specimens with AR-GNP-M25 exhibit

higher crystallinity compared to specimens with AR-GNP-M5. This could be due to larger contact surface of AR-GNP-M25 which provides more nucleation sites for the formation of crystals structures.

On the other hand, there were no significant changes on the melting and crystallisation behaviour for nanocomposites with HT-GNP-M25 compared to AR-GNP-M25. It is uncertain for these phenomena and further in-depth studies will be required to provide answers.

Table 3. DSC data for unfilled PA6 and PA6/GNP nanocomposites

Specimen type	T _c (°C)	T _m (°C)	X (%)
Unfilled PA6	184.3 ± 0.4	218.5 ± 0.4	35.4 ± 0.5
AR-GNP-M5			
3 wt. %	189.9 ± 0.6	219.6 ± 0.5	44.7 ± 1.2
5 wt. %	190.7 ± 0.6	220.0 ± 0.7	46.9 ± 0.4
7 wt. %	191.6 ± 0.7	220.1 ± 0.4	48.3 ± 0.2
14 wt. %	192.6 ± 0.2	221.5 ± 0.2	54.6 ± 1.0
AR-GNP-M25			
3 wt. %	190.1 ± 0.3	219.8 ± 0.7	46.8 ± 1.3
5 wt. %	191.3 ± 0.6	219.8 ± 0.5	49.4 ± 1.5
7 wt. %	192.3 ± 0.8	220.7 ± 0.8	51.1 ± 1.0
14 wt. %	193.3 ± 0.9	221.9 ± 0.1	65.2 ± 0.9
HT-GNP-M25			
3 wt. %	190.0 ± 0.2	220.7 ± 0.7	46.1 ± 0.8
5 wt. %	191.5 ± 0.3	220.9 ± 0.2	48.8 ± 0.8
7 wt. %	192.6 ± 0.9	220.9 ± 0.7	51.3 ± 1.3
14 wt. %	193.2 ± 0.6	221.3 ± 0.3	64.7 ± 0.7

3.2 Damping intensity, $\tan \delta$ and glass transition temperature, T_g

The damping intensity and glass transition temperature, T_g of PA6/GNP nanocomposites were investigated by analysis of the temperature dependencies of $\tan \delta$. Figure 2 shows the $\tan \delta$ curves for unfilled PA6 and PA6/GNP nanocomposites systems. Based on the results obtained, the $\tan \delta$ peak intensity for unfilled PA6 reduced with the addition of GNP. The T_g which was obtained from the $\tan \delta$ peak position also increased slightly with addition of GNP. It is known that the value of $\tan \delta$ at T_g represents the volume of constrained polymer chains within the matrix. The presence of GNP within the matrix hindered the segmental motion of polymer chains thus reduced damping intensity when subjected to cyclic load.

The values of T_g and $\tan \delta$ at T_g are tabulated in Table 2. There were slight improvement in T_g and reduction in $\tan \delta$ at T_g for nanocomposites with AR-GNP-M25 compared to AR-GNP-M5. This may be due to larger flake size of GNP (higher aspect ratio) which could restrict more polymer chains mobility compared to smaller GNP flake size and more energy needed to destroy the constrained polymer chains by the GNP thus increasing the T_g.

More pronounced increased in T_g was observed for nanocomposites with HT-GNP-M25. Eventhough the damping intensity of the $\tan \delta$ peak are higher compared to nanocomposites with AR-GNP-M25, the $\tan \delta$ peak position are at far more higher T_g which could be due to more interactions between the GNP and the matrix. However, further work need to be done to investigate such behavior.

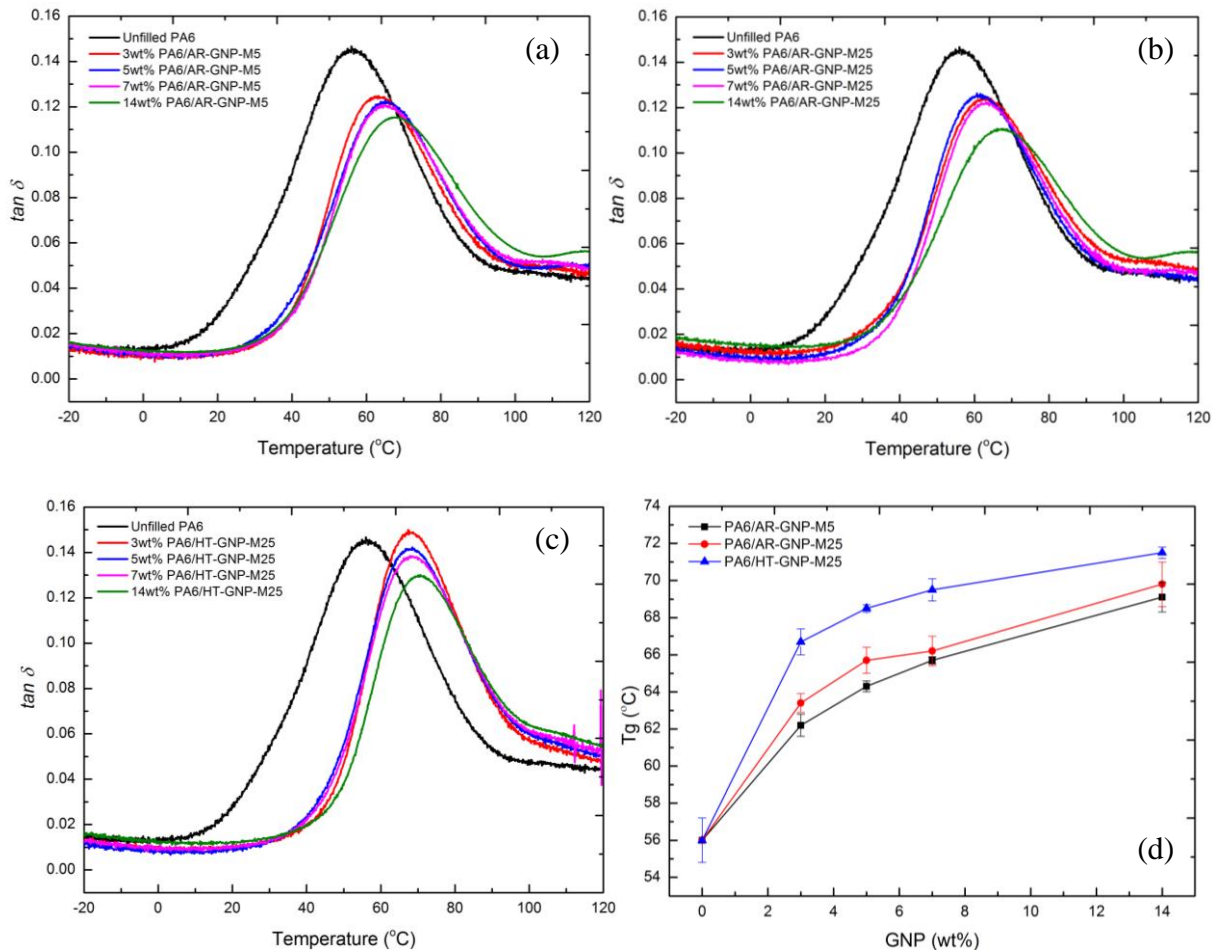


Figure 2. $\tan \delta$ curves for unfilled PA6 and PA6/GNP nanocomposites with (a) AR-GNP-M5 (b) AR-GNP-M25 (c) HT-GNP-M25 and (d) T_g plot of PA6/GNP nanocomposites versus GNP wt.%

Table 2. DMTA data for unfilled PA6 and PA6/GNP nanocomposites

Specimen type	T_g (°C)	$\tan \delta$ at T_g
Unfilled PA6	56.0 ± 1.2	0.147 ± 0.011
AR-GNP-M5		
3 wt.%	62.2 ± 0.6	0.125 ± 0.006
5 wt.%	64.3 ± 0.3	0.121 ± 0.003
7 wt.%	65.7 ± 0.2	0.120 ± 0.001
14 wt.%	69.1 ± 0.8	0.115 ± 0.005
AR-GNP-M25		
3 wt.%	63.4 ± 0.5	0.123 ± 0.005
5 wt.%	65.7 ± 0.7	0.121 ± 0.009
7 wt.%	66.2 ± 0.8	0.120 ± 0.018
14 wt.%	69.8 ± 1.2	0.109 ± 0.006
HT-GNP-M25		
3 wt.%	66.7 ± 0.7	0.149 ± 0.006
5 wt.%	68.5 ± 0.2	0.142 ± 0.009
7 wt.%	69.5 ± 0.6	0.138 ± 0.008
14 wt.%	71.5 ± 0.3	0.129 ± 0.008

3.1 Tensile modulus, E

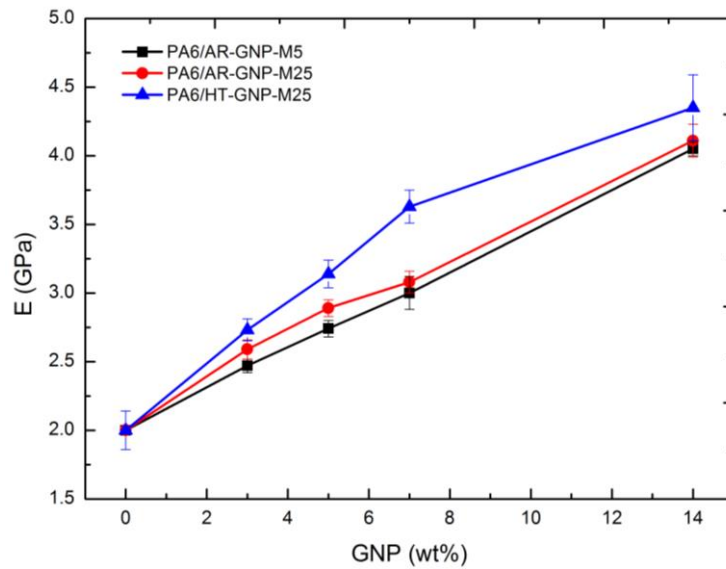


Figure 1: Tensile modulus of PA6/GNP nanocomposites versus GNP wt.%

Figure 1 compares the the tensile modulus of the PA6/GNP nanocomposites with 2 different GNP aspect ratio as well as with heat treated GNP. Details of the tensile modulus values is tabulated in Table 1. It is observed that the tensile modulus of unfilled PA6 improved with addition of GNP and continue to increase wirh increasing GNP addition level. The tensile modulus of the nanocomposites with AR-GNP-M25 are slightly higher compared to AR-GNP-M5. At 5wt.% of GNP, there was 8% increase in tensile modulus with AR-GNP-M25 compared to AR-GNP-M5. This is due to a more extensive contact area of GNP with larger flake diameter providing better interfacial stress transfer with the polymer. However, there was no significance improvement observed at higher weight percentage of GNP and this could be due to formation of aggregates which deteriorates the PA6-GNP interface.

Table 1: Tensile modulus of unfilled PA6 and PA6/GNP nanocomposites

Specimen type	E (GPa)
Unfilled PA6	2.0 ± 0.14
AR-GNP-M5	
3 wt. %	2.47 ± 0.05
5 wt. %	2.67 ± 0.06
7 wt. %	3.00 ± 0.12
14 wt. %	4.05 ± 0.05
AR-GNP-M25	
3 wt. %	2.59 ± 0.07
5 wt. %	2.89 ± 0.06
7 wt. %	3.06 ± 0.08
14 wt. %	4.11 ± 0.12
HT-GNP-M25	
3 wt. %	2.73 ± 0.08
5 wt. %	3.14 ± 0.10
7 wt. %	3.63 ± 0.12
14 wt. %	4.32 ± 0.24

On the other hand, nanocomposites with heat treated GNP (HT-GNP-M25) significantly enhanced the tensile modulus of the unfilled PA6 compared to as received GNP (Ar-GNP-M25). Highest improvement was observed at 7wt.% GNP where there was an 18.5% increment in tensile modulus with HT-GNP-M5 compared to AR-GNP-M25. The improvement with this heat treated GNP may be due to increase exfoliation of the GNP during heat treatment prior to compounding process which result in better dispersion and distribution within the polymer matrix during melt compounding.

4. Conclusions

The presence of GNP within the PA6 matrix significantly enhanced the cooling temperature and crystallinity of the PA6 matrix. Nanocomposites with higher GNP aspect ratio exhibit improved crystallinity due to extensive contact surface which provide more nucleating sites for crystals formation. Addition of GNP into PA6 matrix increase the T_g and impedes the damping intensity. Slight increase in T_g was obtained for nanocomposites with higher GNP aspect ratio but more significant increase was observed with heat treated GNP. The increase in T_g can be attributed to the volume of constrained polymer chains mobility within the matrix. The tensile modulus of unfilled PA6 increased with addition of GNP. Slight increment of tensile modulus was achieved with higher GNP aspect ratio at low GNP wt.% but shows no significant difference at higher wt.%. Nanocomposites with heat treated GNP results in even higher tensile modulus compared to as received GNP. It is assumed that the heat treatment successfully exfoliate the GNP prior to melt compounding. Nonetheless, further investigation needed to support such claim.

References

- [1] K. S. Novoselov, A. K. Geim, S. V. Morozov, D. Jiang, Y. Zhang, S. V Dubunov, I. V. Grigorieva, A. A. Firsov. Electric field in atomically thin carbon films. *Science*, 306:666-669, 2004.
- [2] A. K. Geim, K. S. Novoselov. The rise of graphene. *Nature Materials*, 6:183-190, 2007.
- [3] V. Singh, D. Joung, L. Zhai, S. Das, S. I. Khondaker, S. Seal. Graphene based materials: past, present and future. *Progress in Materials Science*, 56:1178-1271, 2011.
- [4] R. J. Young, I. A. Kinloch, L. Gong, K. S. Novoselov. The mechanics of graphene nanocomposites: a review. *Composites Science and Technology*, 72: 1459-1476, 2012.
- [5] Fukushima H. Graphite nanoreinforcements in polymer nanocomposites. *PhD thesis*, Michigan State University, Department of Chemical Engineering and Materials Science, 2003.
- [6] Kalaitzidou K. Exfoliated graphite nanoplatelets as reinforcement for multifunctional polypropylene nanocomposites. *PhD thesis*, Michigan State University, Department of Chemical Engineering and Materials Science, 2006.
- [7] E. V. Kuvardina, L. A. Novokshonova, S. M. Lomakin, S. A. Timan, I. A. Tchmutin. Effect of the graphite nanoplatelets size on the mechanical, thermal and electrical properties of polypropylene/exfoliated graphite nanocomposites. *Journal of Applied Polymer Science*, 128(3):1417-1424, 2012.
- [8] S. R. Ahmad, R. J. Young, I. A. Kinloch. Raman spectra and mechanical properties of graphene/polypropylene nanocomposites. *International Journal of Chemical Engineering and Applications*, 6:1-5, 2015.
- [9] C. Valles, A. M. Abdelkader, R. J. Young, I. A. Kinloch. The effect of flake diameter on the reinforcement of few-layer graphene-PMMA composites. *Composites Science and Technology*, 111:17-22, 2015.